Vanadium Oxides on Aluminum Oxide Supports. 2. Structure, Vibrational Properties, and Reducibility of V$_2$O$_5$ Clusters on α-Al$_2$O$_3$(0001)

Veronika Brázdová, M. Verónica Ganduglia-Pirovano, and Joachim Sauer*

Humboldt-Universität zu Berlin, Institut für Chemie, Unter den Linden 6, D-10099 Berlin, Germany

The structure, stability, and vibrational properties of isolated V$_2$O$_5$ clusters on the Al$_2$O$_3$(0001) surface have been studied by density functional theory and statistical thermodynamics. The most stable structure does not possess vanadyl oxygen atoms. The positions of the oxygen atoms are in registry with those of the alumina support, and both vanadium atoms occupy octahedral sites. Another structure with one vanadyl oxygen atom is only 0.12 eV less stable. Infrared spectra are calculated for the two structures. The highest frequency at 922 cm^{-1} belongs to a V−O stretch in the V−O−Al interface bonds, which supports the assignment of such a mode to the band observed around 941 cm^{-1} for vanadia particles on alumina. Removal of a bridging oxygen atom from the most stable cluster at the V−O−Al interface bond costs 2.79 eV. Removal of a (vanadyl) oxygen atom from a thin vanadia film on α-Al$_2$O$_3$ costs 1.3 eV more, but removal from a V$_2$O$_5$(001) single-crystal surface costs 0.9 eV less. Similar to the V$_2$O$_5$(001) surface, the facile reduction is due to substantial structure relaxations that involve formation of an additional V−O−V bond and yield a pair of V^{IV}(d^1) sites instead of a V^{III}(d^2)/V^V(d^0) pair.

I. Introduction

Vanadium oxides supported on another metal oxide (e.g., TiO$_2$, ZrO$_2$, and SiO$_2$) are important industrial catalysts used in selective oxidation processes.[1−4] The catalytic activity can change by several orders of magnitude depending on the support and is related to the surface reducibility.[1,5] However, despite considerable work, the nature of the vanadia−support interaction is poorly understood on the atomic scale. This is due to the complexity of the surface structure of the *real* supported catalysts.[6,7] The study of well-defined *model* systems of increasing complexity, both experimental and theoretical, is of importance for analyzing the support effect on the stability, reducibility, and reactivity of the active phase.

Vanadia/alumina model catalysts have been investigated under ultrahigh-vacuum (UHV) conditions.[8−11] Vanadium oxide has been grown on an α-Al$_2$O$_3$(0001) surface,[8] and more recently dispersed vanadia particles (20−30 Å wide and 3−6 Å thick) have been deposited on an ultrathin alumina film.[9] Using infrared (IR) spectroscopy, surface-localized vanadyl groups (V=O) have been identified. The IR spectrum features also a broad band at 941 cm^{-1} that has been assigned to V−O−Al interface species.[10,11] The alumina film itself, grown on a NiAl support, has a structure with 4-fold and 5-fold coordinated Al atoms which is different from all known Al$_2$O$_3$ polymorphs.[12,13]

Theoretically, ultrathin vanadia films (≲1.6 Å) supported on α-Al$_2$O$_3$ (ref 14) and thicker films (up to ∼6 Å) have been considered.[15] The calculations indicate that the presence of surface vanadyl groups is indeed a dominant feature of the termination of the various film structures that may form at a given temperature, depending on oxygen pressure and vanadium concentration. While these models represent alumina-supported vanadia layers or large flat particles, the present study examines models for dispersed aggregates at low vanadia loading.

We investigate V$_2$O$_5$ clusters supported on the α-Al$_2$O$_3$(0001) surface, combining periodic density functional theory (DFT) and statistical thermodynamics. Recently, such a model catalyst supported on clean and hydroxylated TiO$_2$ surfaces has been investigated.[16−20] Different coordinations V$_2$O$_5$ of clusters onto the Al and O surface sites are considered and the most stable identified. The energy costs required to reduce the supported clusters are calculated. Comparison is made with supported vanadia films on α-Al$_2$O$_3$[14,15] to assess possible size effects on the reducibility (that include the existence of differently coordinated sites) and with the clean V$_2$O$_5$(001) surface[21] to evaluate differences due to the presence of the alumina substrate. Special attention will be paid to surface relaxations which play an important role in the reduction.

We also compare the stability of the supported vanadia (V$_2$O$_5$ and V$_2$O$_4$) clusters with the stability of differently terminated vanadia films on the α-Al$_2$O$_3$(0001) surface.[15] We do this for different temperatures and different preparation conditions (oxygen pressure and vanadium supply) by means of a phase diagram. We also characterize the supported clusters by their vibrational frequencies.

II. Methods

Density functional theory with the gradient-corrected Perdew−Wang exchange-correlation functional (PW91)[22,23] as implemented in the Vienna ab initio package (VASP)[24,25] was used. The core electrons were described by the projector augmented-wave (PAW) method.[26,27] The core radii for Al, V, and O atoms were 1.90, 2.30, and 1.52 au, respectively. A plane-wave basis set was used with a kinetic energy cutoff of 400 eV. The Brillouin zone was sampled using Monkhorst-Pack grids.[28] The particular *k*-point set is given in the description of each system. All atoms were allowed to relax in all systems

* To whom correspondence should be addressed: e-mail sek.qc@chemie.hu-berlin.de.

Vanadium Oxides on Aluminum Oxide Supports

J. Phys. Chem. B, Vol. 109, No. 49, 2005 **23533**

TABLE 1: Changes in the Interlayer Spacings of the Clean α-Al$_2$O$_3$(0001) Surface and the Surface with the Chemisorbed L1 Cluster Relative to the Bulk Truncated Geometry of α-Al$_2$O$_3$(0001)^a

	Al$_2$O$_3$(0001)		L1^b	
	[Å]	[%]	[Å]	[%]
Al^1−O^2	−0.73	−86	−0.25	−29
O^2−Al^3	+0.03	+4	+0.07	+9
Al^3−Al^4	−0.27	−45	−0.19	−39
Al^4−O^5	+0.17	+20	+0.12	+14
O^5−Al^6	+0.04	+5	+0.00	+0
Al^6−Al^7	−0.03	−7	+0.03	+6
Al^7−O^8	+0.01	+1	−0.02	−2
O^8−Al^9	−0.02	−2	−0.01	−2
Al^9−Al^{10}	+0.04	+8	+0.03	+5
Al^{10}−O^{11}	−0.02	−2	−0.01	−2

^{a} The changes in the bottom half of the slab with the supported cluster differ by at most by 1% from the clean slab. ^{b} Averaged values.

until the total energy change was smaller than 10^{-5} eV. This criterion leads to forces smaller than 0.01 eV/Å. The vibrational modes were obtained by finite differences of the forces, with the atomic displacement 0.02 Å at a 400 eV cutoff. No imaginary frequencies were found.

The rhombohedral cell of bulk α-Al$_2$O$_3$ was optimized using the stress tensor algorithm implemented in VASP with an 800 eV cutoff and a $(4 \times 4 \times 4)$ k-point mesh. The optimized parameters ($a = 5.176$ Å and $\beta = 55.31°$) differ from the experimental values[29] by less than 1%. The corresponding lattice parameters of the hexagonal cell are $a = 4.804$ Å and $c = 13.108$ Å.

III. Models

A. Al$_2$O$_3$(0001) Support. The atoms in the hexagonal unit cell of α-alumina (corundum) are stacked along the [0001] direction in 12 planes of Al atoms and six planes of O atoms in a sequence Al−O$_3$−Al−Al−O$_3$−Al−...−Al, with oxygen atoms in an almost hexagonal close-packed stacking and Al in the resulting interstitial sites. Al atoms occupy two-thirds of the available octahedral sites and are hexagonally arranged (in one of the three types of hexagonal networks, which differ in the position of the vacant octahedral sites). In the following, the term *trilayer* is used for the repeating Al−O$_3$−Al unit. The hexagonal unit cell includes six such trilayers. The clean Al$_2$O$_3$-(0001) surface terminated by a single Al layer has no dipole moment in the (0001) direction and is the most stable one.[30−32] To model it, we use a six-trilayer (0001) oriented slab (supercell approach) in the hexagonal cell with a vacuum region of ∼6 Å ($c = 18$ Å). The mesh is $(4 \times 4 \times 1)$. Table 1 lists distances between the atomic planes in the relaxed system, relative to the bulk truncated geometry. The atomic planes are denoted by superscripts, e.g., Al^1, O^2, Al^3, etc. The top Al^1 plane relaxes inward by 87%, while the second O^2 plane relaxes slightly outward, so that it is almost in one plane with the surface Al atoms. The results are very similar to those obtained by other periodic DFT calculations, and they have been discussed elsewhere.[14] This slab is used to model the α-Al$_2$O$_3$ support for the V$_2$O$_5$ clusters.

B. V$_2$O$_5$ and V$_2$O$_4$ Clusters and O$_2$ Molecule. DFT calculations on V$_2$O$_5$ clusters in the gas phase predict two stable structures: a linear and a cyclic one (see Figure 1a,b).[33−36] The linear cluster (C_2 point group) has four single coordinated oxygen atoms (vanadyl oxygens, O$^{(1)}$) and one doubly coordinated oxygen atom (bridging oxygen, O$^{(2)}$). The cyclic cluster (C_s point group) has three vanadyl oxygen atoms and two
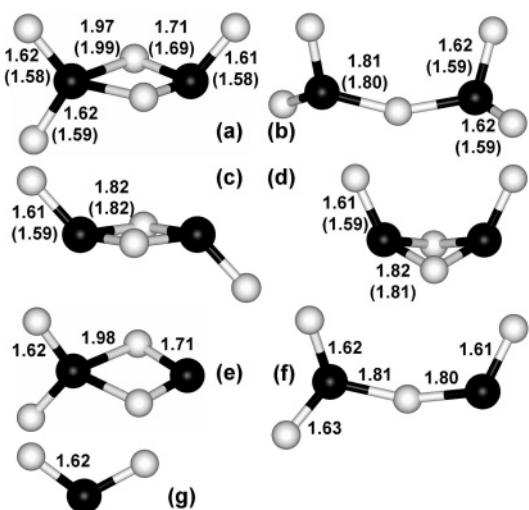

Figure 1. Gas-phase vanadia clusters. (a) V$_2$O$_5$ cyclic cluster, (b) V$_2$O$_5$ linear cluster, (c) V$_2$O$_4$ cyclic cluster trans configuration, (d) V$_2$O$_4$ cyclic cluster cis configuration, (e) V$_2$O$_4$ cyclic cluster with two vanadyl bonds on one V atom (VO$_2$V(O)O), (f) V$_2$O$_4$ linear cluster (OVOV(O)O), and (g) VO$_2$ cluster. Bond lengths (in Å) as calculated in this work. Bond lengths in parentheses are from all-electron calculations, refs 34 and 37 for the V$_2$O$_5$ and V$_2$O$_4$ clusters, respectively.

bridging oxygen atoms. The bridging oxygen atoms and the vanadium atoms form a V−O$^{(2)}$−V−O$^{(2)}$ ring.

The clusters were placed in a cubic cell with $a = 10$ Å, and the Γ point was used. The cyclic cluster is by 0.96 eV more stable than the linear one. This is in agreement with an all-electron calculation (B3LYP functional, TZVP basis set),[33] which gives a total energy difference of 0.81 eV. Our calculations give bond lengths systematically longer by 0.01−0.04 Å (cf. Figure 1).

We also considered V$_2$O$_4$ clusters in the gas phase, which are the reference for evaluating the adsorption energy of reduced V$_2$O$_5$ clusters. According to multireference wave function-based calculations,[37] the most stable configuration has a four-membered V−O$^{(2)}$−V−O$^{(2)}$ ring and two vanadyl oxygen atoms in the trans configuration. There is one d electron at each of the two V atoms. Their spins form an open-shell singlet state which is about 93 meV below the corresponding triplet state. All-electron B3LYP calculations give qualitatively the same result, with the open-shell singlet 112 meV below the triplet.[37] The energy of the low-spin states was obtained from the energies of the broken symmetry solution and the triplet state at the same geometry. The present calculations predict the open-shell singlet state 177 meV below the triplet state. Figure 1 shows the calculated distances of the vanadyl (V=O) and the V−O$^{(2)}$ bonds (1.61 and 1.82 Å, respectively) and compares them with previous B3LYP results.[33]

The cis isomer is less stable than the trans isomer (Table 2). Note that with the PW91 functional a broken symmetry solution is not found for this isomer, and the energy of the open-shell singlet state cannot be obtained.

Two other less stable V$_2$O$_4$ isomers are a cyclic V^{III}O$_2$V^V-(O)O cluster with two vanadyl bonds on one V atom and none on the other and a linear OV^{III}OV^V(O)O cluster (see Figure 1, e and f, respectively). They are 0.92 and 1.77 eV, respectively, less stable than the open-shell singlet V$_2$O$_4$ trans structure. The electronic ground state of these clusters is a triplet with a V^{III}-(d^2)/V^V(d^0) electron configuration. Two VO$_2$ species are 4.70 eV less stable than the trans V$_2$O$_4$ cluster.

The total energy of the isolated O$_2$ molecule, which is involved in the calculation of the oxygen vacancy formation

TABLE 2: Total Energy Differences (in eV) of Different V$_2$O$_4$ Gas Phase Clusters

cluster	spin state	PW91/ PAW[a]	B3LYP/ AE[b]
V$_2$O$_4$ cyclic trans	singlet open shell	0[c]	0
V$_2$O$_4$ cyclic trans	triplet B$_u$	0.177	0.112
V$_2$O$_4$ cyclic cis	singlet open shell		0.169
V$_2$O$_4$ cyclic cis	triplet B$_2$	0.257	0.257
V$_2$O$_4$ linear (OVOV(O)O)	triplet	1.765	
V$_2$O$_4$ cyclic (VO$_2$V(O)O)	triplet	0.920	
2 VO$_2$	2× doublet	4.704	

[a] This work. PW91 functional, PAW, plane waves. *[b]* Reference 37. B3LYP functional, all electron calculations, TZVP basis set. *[c]* The projection was done assuming $\langle \hat{S}^2 \rangle = 1$.

energy, has been calculated in a tetragonal cell of side lengths $a = 10$ Å, $b = 11$ Å, and $c = 12$ Å with Γ-point sampling of the Brillouin zone (other parameters as described above). The binding energy in O$_2$ is 3.13 eV per O atom and the bond distance 1.235 Å. The experimental results are 2.59 eV/atom (obtained after adding the contributions due to zero-point vibrations to the $T = 0$ K value) and 1.207 Å.[38] The overestimation of the binding energy and the bond distance are in line with earlier density functional calculations that used gradient corrected functionals.[36,39,40] Sauer and Döbler have shown that this overestimation does not change relative values of oxygen vacancy formation energies.[36]

C. Adsorbed V$_2$O$_5$ Clusters. A (2×2) α-Al$_2$O$_3$(0001) surface unit cell (9.608 Å × 9.608 Å) with a vacuum region of 11 Å ($c = 23$ Å) was used. The V$_2$O$_5$ clusters were placed above the surface on one side of the slab so that the closest distance between the cluster and the surface was longer than 2.0 Å. There are two V atoms per four surface Al atoms in the (2×2) cell. A $(2 \times 2 \times 1)$ k-point mesh was used. Initial guesses for different adsorption geometries were obtained by considering the relative positions of the clusters' O atoms and the atoms in the first four atomic planes of the clean surface. These planes are Al^1, O^2, Al^3, and Al^4 (see below). Additionally, selected configurations were used as initial structures in a short finite temperature molecular dynamics (MD) simulation[41] followed by a relaxation performed within the quasi-Newton scheme.

For the purpose of preselecting the more stable adsorbed V$_2$O$_5$ clusters, ultrasoft pseudopotentials[42] with a cutoff of 250 eV were used. Core radii of these pseudopotentials were 2.65, 2.40, and 1.90 au for Al, V, and O atoms, respectively. With these computational parameters the geometries of the gas-phase V$_2$O$_5$ clusters and of the V$_2$O$_5$/Al$_2$O$_3$ systems are comparable with those obtained at higher accuracy. In particular, for the gas-phase clusters bond lengths differ by less than 0.02 Å. Moreover, the total energy differences of different optimized V$_2$O$_5$/Al$_2$O$_3$ systems are qualitatively the same as those obtained using PAW potentials and a 400 eV cutoff (see section 4).

Linear V$_2$O$_5$ Clusters. They can be positioned above the surface so that either three, two, or none of the vanadyl bonds point toward the surface (see Figure 2). If three vanadyl bonds point initially toward the surface, two oxygen atoms lie directly above Al atoms from the same plane, while the third oxygen atom is above an Al atom from a different plane. These configurations will be denoted here LAl^{j}Al^{k}Al^k, where j and k can be 1, 3, or 4 and $j \neq k$. The fourth vanadyl bond points away from the alumina surface. Six such structures can be constructed.

If none of the vanadyl bonds point toward the surface, the bridging oxygen atom and two vanadyl oxygen atoms are about the same distance from the surface and will be included in the

notation, namely LAl^{j}Al^{k}Al^l, where $j \neq k \neq l$ and j, k, l can be either 1, 3, or 4. The middle number indicates the position of the bridging oxygen and the first and third one the positions of the vanadyl oxygen atoms above the surface Al atoms (see Figure 2). Three such structures can be generated.

The case with two vanadyl bonds pointing down is denoted LAl^{j}Al^j, with $j = 1$, 3, or 4. This notation indicates above which Al atoms from the surface (i.e., Al^1, Al^3, or Al^4) are the two O atoms from the cluster located. The LAl^{1}Al^1 and the LAl^{1}Al^4-Al^4 structures were also considered as a starting point for the simulated annealing runs. In total, 12 starting structures with the linear clusters have been considered.

Cyclic V$_2$O$_5$ Cluster. The cluster was put above the alumina surface so that two or one vanadyl bond was pointing down. In the former case the four-membered ring was approximately parallel to the alumina surface. The two vanadyl oxygens closest to the surface were positioned either both above Al surface atoms (the notation is CAl^{j}Al^k, now j can be equal to k; see Figure 3 for an example) or one above an Al atom and the other above a 6-fold hollow site (CAl^{j}h^6) or both above hollow sites (Ch^{6}h^6).

In the case of one vanadyl bond pointing down, the four-membered ring was slightly tilted, so that the V atom which has only one vanadyl bond (V′) was closer to the surface. The O atom closest to the surface was positioned above an Al atom and the V′ atom either above a surface oxygen atom (CAl^{j}O^2, see Figure 3) or above a 6-fold hollow site (CAl^{j}h^6). In total, 16 initial configurations with the cyclic cluster were constructed.

IV. Results and Discussion

Tables 3 and 4 list relative energies of all considered linear and of the most stable cyclic V$_2$O$_5$/Al$_2$O$_3$ systems, respectively. The calculated relative V$_2$O$_5$ adsorption energies using ultrasoft pseudopotentials and a 250 eV cutoff and those using PAW potentials and 400 eV follow the same trend. The only exception is the LAl^{4}Al^{3}Al^1 system for which the higher accuracy led to the formation of an additional bond. Thus, only linear structures that, at the lower accuracy, are not more than ∼1 eV above the most stable configuration and selected adsorbed cyclic clusters were further optimized at higher accuracy. Figure 4 shows the optimized structures of the most stable configurations.

A. Adsorbed Linear V$_2$O$_5$ Cluster. The most stable system is the adsorbed LAl^{1}Al^{4}Al^4 cluster. It will be denoted L1. The optimization of four other initial structures (LAl^{4}Al^{1}Al^1, LAl^3-Al^{4}Al^1, LAl^{4}Al^{3}Al^1, and LAl^{4}Al^4) leads to virtually the same final geometry that is less stable by ∼0.1 eV and will be denoted L2.

The general observation is that a V$_2$O$_5$ unit would bind as much as possible to the surface, so that the undercoordinated surface Al and O atoms can increase their coordination (see Table 5). The most stable L1 system has four V−O$^{(2)}$−Al^1 bonds and one V−O$^{(3)}$−V,Al^1 bond. O$^{(2)}$ denotes a 2-fold coordinated oxygen atom in both V−O$^{(2)}$−V and V−O$^{(2)}$−Al bridges, and O$^{(3)}$ indicates a 3-fold coordinated oxygen atom. However, it does not have any vanadyl group. All Al^1 atoms are thus "occupied". One V atom (V1) occupies the octahedral site above an Al^4 atom that Al atoms would occupy in bulk Al$_2$O$_3$; however, it is 5-fold coordinated (see Table 5). The V2 atom above an Al^3 atom is also 5-fold coordinated but occupies a vacant octahedral site instead. The oxygen atoms are approximately in a plane parallel to the surface at positions that are in registry with those of the support; i.e., they follow the hexagonal stacking of the oxygen layers. However, the oxygen
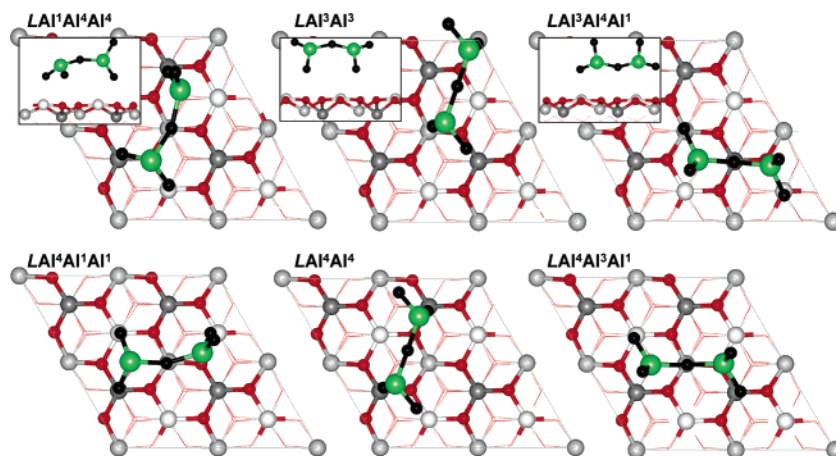
Figure 2. Initial configurations for linear V_2O_5 clusters above α-Al_2O_3(0001). Oxygen and vanadium atoms of the cluster are black and green, respectively. Oxygen atoms of the alumina slab are red. Al^1, Al^3, and Al^4 atoms are white, medium gray, and gray, respectively. The atoms from the plane O^5 and beneath are drawn as lines. The left column corresponds to clusters with three vanadyl bonds pointing down. Configurations with two or no vanadyl atoms approaching the surface are shown in the middle and right column, respectively (see text).
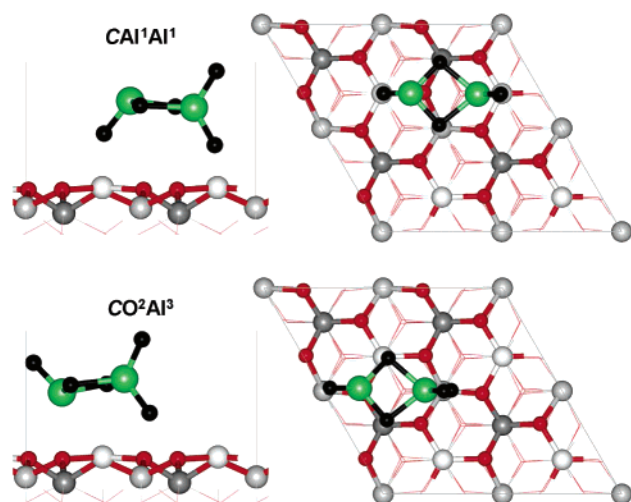

Figure 3. Examples of initial configurations for cyclic clusters above α-Al_2O_3(0001). CAl^jAl^k, $j = k = 1$ (top) and CO^2Al^j, $j = 3$ (bottom). The color code is the same as in Figure 2.

"plane" is in this case much closer to the V atoms than an oxygen plane would be to the Al atoms in bulk α-Al_2O_3. Adsorption of the V_2O_5 cluster induces lattice relaxations that cause buckling of the atomic planes of the support (see Figure 4) and result in an overall expansion of the outermost interlayer spacings. In Table 1 averaged interlayer spacings are listed. The larger changes are found for the first interlayer distance with an expansion of $\sim$60% with respect to the clean surface.

For the second most stable L2 clusters, one of their V atoms (V1, see Figure 4) is above an Al^4 atom, as in the most stable system, but it is 6-fold coordinated, and the other is above an O^2 atom and is tetrahedrally coordinated. There are three $V-O^{(2)}-Al^1$ bonds, one $V-O^{(2)}-V$ bond, and one $V=O^{(1)}$ bond. The oxygen atoms that are bound to the support are at positions similar to those for the L1 cluster. The total energy difference between the L1 and L2 clusters is 0.12 eV. The correction for zero-point vibration changes this difference to 0.13 eV and can therefore be neglected.

The optimized LAl^3Al^3 structure (denoted L3) is 0.62 eV less stable than the L2 clusters. It possesses one vanadyl bond. Its V2 atom is above an O^2 atom and is 4-fold coordinated, while the V1 atom occupies a vacant tetrahedral site (above an Al^3 atom, not Al^4) and is 5-fold coordinated (see Figure 4). The calculated bond lengths differ by no more than 0.02 Å for most

TABLE 3: Relative Energies ΔE (in eV) of the Adsorbed Linear Clusters with Respect to the Most Stable System

starting structure	final structure	$\Delta E/250^a$	$\Delta E/400^b$
three vanadyl bonds initially pointing down			
$LAl^1Al^3Al^3$		3.4	
$LAl^1Al^4Al^4$	L1	0^c	0^c
$LAl^1Al^4Al^{4d}$		2.8	
$LAl^3Al^4Al^1$		2.1	
$LAl^3Al^4Al^4$		2.8	
$LAl^4Al^1Al^1$	L2	0.1	0.12^e
$LAl^4Al^3Al^3$		3.5	
$2O^{(1)}$ and $1O^{(2)}$ atoms initially at the same distance from the surface			
$LAl^3Al^4Al^1$	L2	0.2	0.12^e
$LAl^4Al^1Al^3$		2.1	
$LAl^4Al^3Al^1$	L2	1.1	0.12^e
two vanadyl bonds initially pointing down			
LAl^1Al^1		3.6	
$LAl^1Al^{1\ d}$	L4	0.7	0.78
LAl^3Al^3	L3	0.8	0.74
LAl^4Al^4	L2	0.2	0.12^e

^{a} Ultrasoft pseudopotentials. Cutoff 250 eV. ^{b} PAW. Cutoff 400 eV. ^{c} Reference point. ^{d} MD optimization. ^{e} Optimized structures $LAl^4Al^1Al^1$, $LAl^3Al^4Al^4$, $LAl^4Al^3Al^1$, and $LAl^1Al^4Al^4$ are virtually identical.

TABLE 4: Relative Energies ΔE (in eV) of the Adsorbed Cyclic Clusters with Respect to the Most Stable System, Which Is the Optimized Adsorbed Linear Cluster L1

starting structure	final structure	$\Delta E/250^a$	$\Delta E/400^b$
two vanadyl bonds initially pointing down			
CAl^1Al^1		1.7	1.62
CAl^1Al^3		5.8	
CAl^1h^6		1.8	1.75
Ch^6h^6		1.9	1.86
one vanadyl bond initially pointing down			
CAl^1O^2		2.7	2.50
CAl^3O^2	C2	1.1	1.04
CAl^3h^6	C1	1.1	1.04
CAl^4h^6		1.9	1.61

^{a} Ultrasoft pseudopotentials. Cutoff 250 eV. ^{b} PAW. Cutoff 400 eV.

bonds compared to L2, except for the bonds between the V1 atom and the O atoms of the substrate. The difference for the latter is at least twice as large. It is likely that the fault in the stacking and the reduced coordination of the V1 atom causes the energy difference.

The structures obtained from the initial configurations LAl^1-Al^1 and $LAl^1Al^4Al^4$ after the relatively short (3 ps) simulated
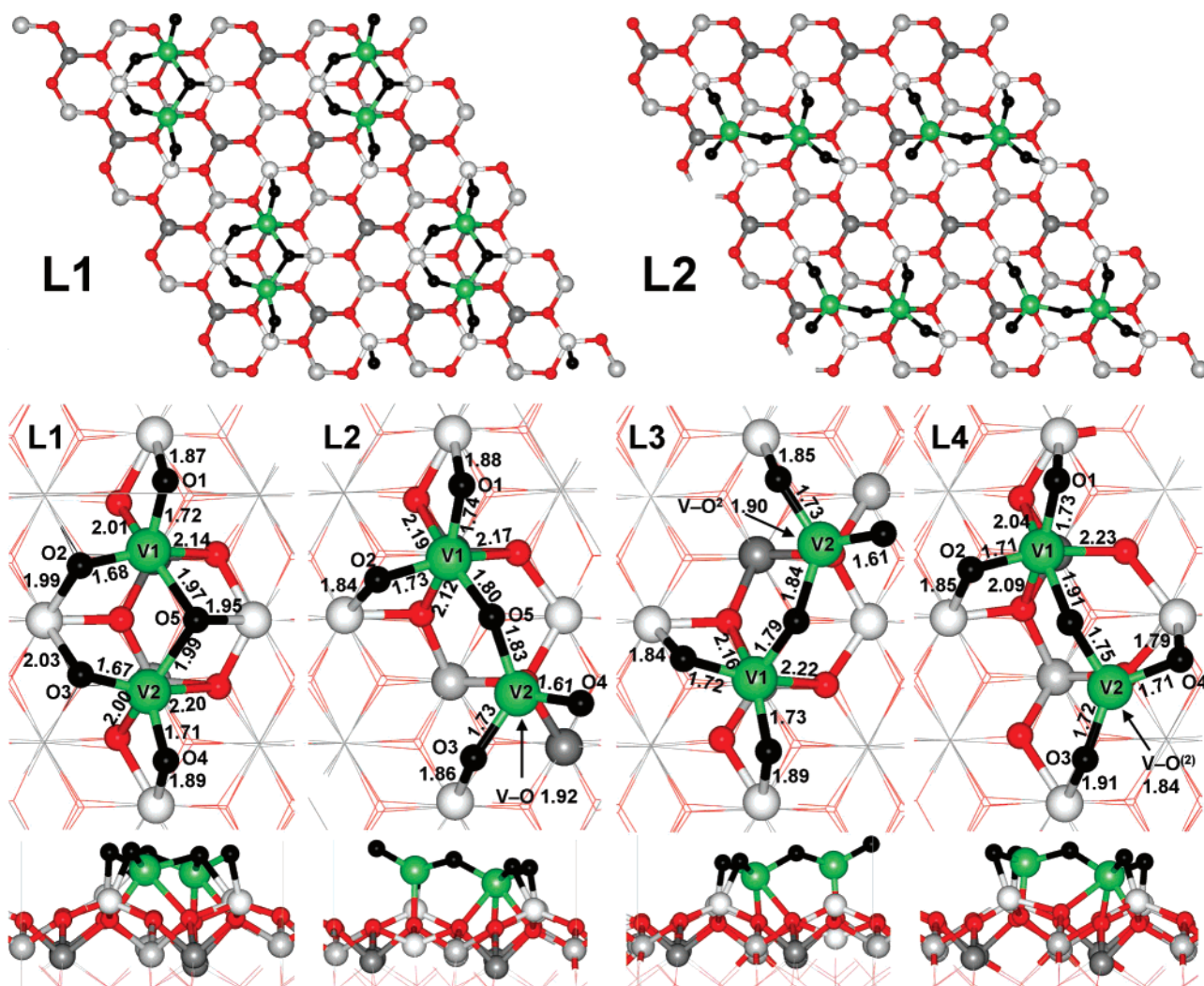
Figure 4. Optimized structures of the adsorbed linear V_2O_5 cluster. The color code is the same as in Figure 2. Bond lengths are in Å.

TABLE 5: Coordination of Atoms in the Al_2O_3 and V_2O_5/Al_2O_3 Species

	$Al_2O_3(0001)$	L1	L2	L3	L4	C1	C2
Al^1	all 3	$1 \times 5, 3 \times 4$	$3 \times 4, 1 \times 3$	$3 \times 4, 1 \times 3$	all 4	$3 \times 4, 1 \times 3$	$3 \times 4, 1 \times 3$
O^2	all 3	$4 \times 4, 8 \times 3$	$4 \times 4, 8 \times 3$	$3 \times 4, 9 \times 3$	$4 \times 4, 8 \times 3$	$3 \times 4, 9 \times 3$	$3 \times 4, 9 \times 3$
		5(oct)[a]	6(oct)	5(vac)	6(oct)	6(oct)	6(oct)
V2		5(vac)[b]	4(on-top O^2)[c]	4(on-top O^2)	4(on-top O^2)	4(vac)	4(vac)
$V=O^{(1)}$		0	1	1	0	2	1
$V-O^{(2)}-Al$		4	3	3	4	1	2
$V-O^{(2)}-V$		0	1	1	1	0	1
$V-O^{(3)}-V,Al$		1	0	0	0	2	1
ΔE^d		0.00	0.12	0.74	0.78	1.04	1.04

[a] An octahedral site that would be occupied in bulk α-Al_2O_3. [b] An octahedral site that would be vacant in bulk α-Al_2O_3. [c] Above an O^2 surface atom. [d] Total energy difference (in eV) with respect to L1.

annealing runs and a subsequent structure optimization ($T = 0$ K) did not have energies lower than L1. They are about 0.7 and 2.8 eV, respectively, less stable (calculated at the lower accuracy). The former was further optimized at the higher accuracy, and the final L4 structure (Figure 4) is 0.66 eV above the L2 cluster. In the L4 structure, as in L2, V1 is octahedrally coordinated above Al^4 and the V2 atom is coordinated to an O^2 site. There is one $V-O^{(2)}-V$ bridge and four (instead of three) $V-O^{(2)}-Al^1$ bonds. Hence, there is no free vanadyl group left in the final structure. Because of the additional $V-O^{(2)}-Al^1$ bond, the final L4 structure is distorted compared to L2 (see Figure 4). In particular, the O5-V2-O4 angle is by 10° narrower and rotated with the O4 atom (the vanadyl oxygen in L2) toward the surface Al atom, enabling the bond formation.

The V2-O4 bond is 0.1 Å longer than the vanadyl bond in L2. The positions of most of the oxygen atoms of this cluster are laterally displaced from those following the hexagonal stacking of the oxygen layers. Moreover, the "plane" formed by the oxygen atoms is buckled. Ultimately, keeping the vanadyl bond means less distortion and stabilizes the structure.

Summarizing, V atoms prefer to occupy octahedral sites (that may correspond either to an occupied or a vacant site of the bulk stacking) in which their coordination to O atoms can be largest (cf. Table 5), while O atoms remain almost in one plane occupying sites that maximize the O-O lateral ion spacing. Moreover, most of the oxygen atoms at the interface between vanadia and the alumina support are 2-fold coordinated ($V-O^{(2)}-Al^1$). This is different from the models for Al_2O_3 supported
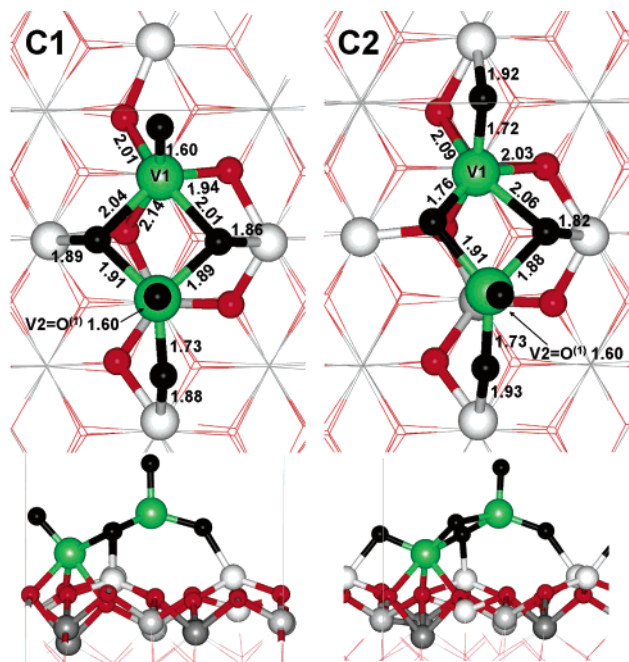
Figure 5. Optimized structures of the adsorbed cyclic V_2O_5 clusters C1 (left) and C2 (right). The color code is the same as in Figure 2. Bond lengths are in Å.

vanadia films,[14,15] which contain 3-fold coordinated oxygen atoms at the interface only.

B. Adsorbed Cyclic V_2O_5 Cluster. Cyclic V_2O_5 clusters are about 1 eV less stable than the most stable system (L1, see Table 4). This is not surprising because the cyclic cluster itself is stabilized by the $V-O^{(2)}-V-O^{(2)}$ ring, and therefore it does not bind so strongly to the substrate. The two systems with a relative energy of 1.04 eV have only slightly different structures (CAl^3h^6 and CAl^3O^2, see Figure 5). They will be denoted C1 and C2, respectively. Both systems have one 6-fold coordinated V atom (V1) in the octahedral site above Al^4 and one 4-fold coordinated (V2) in the vacant site above Al^3. Note that due to the presence of the ring, not all of the oxygen atoms are in registry with those of the Al_2O_3 support. In C1 both O atoms in the ring are bound to surface Al^1 atoms, so that they are 3-fold coordinated. One of the originally vanadyl O atoms is bound to an Al^1 atom, forming a $V-O^{(2)}-Al^1$ bridge. The system has two single coordinated oxygen atoms. The C2 system, on the other hand, has only one vanadyl oxygen, two $V-O^{(2)}-Al^1$ bridges, and one 3-fold coordinated O atom, whereas the other O atom in the ring does not bind to substrate atoms. In summary, the placement of V atoms is the same as in the most stable adsorbed linear cluster. The tendency to bind to the substrate as much as possible by forming bridges is also similar for both the linear and cyclic clusters. However, the rigidity imposed by the ring results in considerably less stable systems which will therefore not be discussed any further.

C. Stability and Comparison with TiO_2-Supported V_2O_5 Clusters. The V_2O_5 cluster adsorption energy can be defined as

$$E_{ad} = E(Al_2O_3)_{solid} + E(V_2O_5)_{gas} - E(V_2O_5/Al_2O_3)_{solid} \quad (1)$$

where positive values indicate an exothermic process. $E(V_2O_5/Al_2O_3)_{solid}$, $E(Al_2O_3)_{solid}$, and $E(V_2O_5)_{gas}$ are the total energies of the slab with the supported cluster, the clean support slab, and the most stable (cyclic) V_2O_5 cluster in the gas phase, respectively.

The adsorption energies of the L1 and L2 clusters on a (2 × 2) α-Al_2O_3(0001) surface unit cell are 6.80 and 6.67 eV. The coverage is two V atoms per four surface Al atoms (i.e., 0.5 monolayers (ML)), and the surface unit cell has an area of 80 Å^2. A similar value (6.43 eV) has been obtained for the adsorption of V_2O_5 clusters on the unreconstructed (anatase) titania (001) surface in a (3 × 2) surface unit cell.[16,17] Although there are two V atoms per six surface Ti atoms in this system (i.e., 1/3 ML), the (3 × 2) surface area (86 Å^2) is comparable to that of our (2 × 2) cell. Indeed, using a (2 × 2) TiO_2(001) surface unit cell (area 57 Å^2), the V_2O_5 adsorption energy decreases by 1.24 eV due to a larger overlap between the V_2O_5 units. Consequently, adsorption of V_2O_5 units on the (3 × 2) TiO_2(001) and (2 × 2) (0001) surfaces, even though the former has six Ti surface atoms and the latter four Al atoms, yields a similar dispersion of the clusters. The adsorption energies of the L1 and L2 clusters dispersed on (2 × 2) α-Al_2O_3(0001) are only by 0.27 and 0.15 eV larger than that of the most stable cluster on a (3 × 2) TiO_2(001) surface. On the clean (3 × 2) TiO_2(001) surface all six Ti atoms are 5-fold coordinated and all six O atoms 2-fold coordinated (in the bulk 6- and 3-fold, respectively). Upon V_2O_5 cluster adsorption only one Ti atom and one surface O atom "gain" one bond each. On the clean (2 × 2) Al_2O_3(0001) surface each of the four surface Al atoms is missing three bonds compared to the bulk, i.e., is 3-fold coordinated, and each of the 12 O atoms has one bond less. Upon cluster adsorption five new Al−O bonds are created as well as four new V−O bonds (cf. Table 5).

D. Adsorbed V_2O_4 Clusters. Concerning the function of the supported vanadia catalysts in oxidation reactions, isotopic labeling studies indicated the participation of lattice oxygen atoms as reactive intermediates.[43,44] Moreover, mechanistic studies have shown that reduced V centers (V^{III} or V^{IV}) are present during steady-state catalysis[45,44] and that the extent of reduction of vanadium oxides during catalytic oxidation correlates with turnover frequencies (see e.g. refs 46 and 47). Thus, the ease of oxygen removal from the supported catalyst is a property of interest. Also, an understanding of the effect of the support on the reducibility of vanadia particles appears desirable in view of the observed variations in catalytic activity with the type of support.[1,5]

In the following we consider the initial reduction of the two most stable supported clusters, namely L1 and L2 by removing each of the five oxygen atoms. The stability difference between L1 and L2 is only ~0.1 eV, suggesting that both structures may form during vanadium evaporation on the alumina substrate at finite temperatures. Table 6 summarizes the calculated oxygen defect formation energies

$$E_b = E(V_2O_4/Al_2O_3)_{solid} - E(V_2O_5/Al_2O_3)_{solid} + \frac{1}{2}E(O_2)_{gas} \quad (2)$$

where positive values indicate an endothermic process. $E(V_2O_4/Al_2O_3)_{solid}$ and $E(O_2)_{gas}$ are the total energies of the slab with the supported reduced cluster and the free oxygen molecule, respectively. To assess the effect of structure relaxations on defect formation energies, Table 6 also shows E_b values for unrelaxed geometries upon oxygen removal.

We first discuss the reduction of the most stable L1 cluster. The structures resulting from removal of the 2-fold coordinated O1 and O2 atoms (bound to the V1 site) are virtually the same (cf. Figure 6). They undergo a significant rearrangement upon reduction that is accompanied by a ~2.6 and 1.6 eV decrease in the vacancy formation energy, respectively. In particular,

TABLE 6: Oxygen Vacancy Formation Energy $E_b(^1/_2O_2)$ (in eV per $^1/_2O_2$ Molecule) for the Relaxed and Unrelaxed Defect Structures Investigated and Reduced Clusters' Adsorption Energy E_{ad} (eV)

system	O vacancy type	$E_b^{unrelax}$ $(^1/_2O_2)$	E_b $(^1/_2O_2)$	$E_{ad}{}^a$
L1−O5	V−O$^{(3)}$−V,Al	5.33	4.75	4.81
L1−O1	V−O$^{(2)}$−Al	5.38	2.79	6.77
L1−O2	V−O$^{(2)}$−Al	4.36	2.80	6.77
L1−O3	V−O$^{(2)}$−Al	4.31	3.31	6.25
L1−O4	V−O$^{(2)}$−Al	5.34	4.51	5.06
L2−O3	V−O$^{(2)}$−Al	5.66	4.77	4.67
L2−O1	V−O$^{(2)}$−Al	5.49	4.53	4.92
L2−O2	V−O$^{(2)}$−Al	5.08	4.41	5.04
L2−O5	V−O$^{(2)}$−V	5.47	3.70	5.74
L2−O4	V=O$^{(1)}$	4.06	3.77	5.68
$^1/_2$V$_2$O$_5$·$^{11}/_2$Al$_2$O$_3{}^b$	V=O$^{(1)}$	4.14	4.11	
V$_2$O$_5$(001)^c	V−O$^{(2)}$−V	5.09, 5.09	3.62, 3.68	
V$_2$O$_5$(001)^d	V−O$^{(3)}$−2V	4.40, 4.45	3.94, 4.00	
V$_2$O$_5$(001)^e	V=O$^{(1)}$	3.76	1.93	
OVO$_2$VO (cyclic)^f	V=O$^{(1)}$		2.77	
OVOV(O)O (linear)^f	V−O$^{(2)}$−V		4.53	

^{a} Adsorption energy with respect to the clean α-Al$_2$O$_3$ surface and the gas-phase V$_2$O$_4$ cluster. ^{b} Reference 15. $E_b(^1/_2O_2)$ for $^1/_4$ ML of the terminating vanadyl oxygen atoms removed from a thin V$_2$O$_3$ film supported on Al$_2$O$_3$. The same computational details as in this work. ^{c} Reference 21. $E_b(^1/_2O_2)$ for $^1/_4$ ML of (the two inequivalent) O$^{(2)}$ defects at the V$_2$O$_5$(001). ^{d} Reference 21. $E_b(^1/_2O_2)$ for $^1/_4$ ML of the (two inequivalent) O$^{(3)}$ defects at the V$_2$O$_5$(001). ^{e} Reference 21. $E_b(^1/_2O_2)$ for $^1/_6$ ML vanadyl oxygen defects at the V$_2$O$_5$(001) surface. DFT/PW91. ^{f} With respect to the gas-phase cyclic V$_2$O$_5$ cluster.

when the O1 atom is removed, the O2 atom moves into the vacant O1 site, and in turn the 2-fold coordinated O3 atom moves toward the V1 atom and becomes 3-fold coordinated. As a result, a second V−O$^{(3)}$−V bridge is formed which creates a four-membered V−O$_2{}^{(3)}$−V ring. The coordination of the V1 increases from 5 to 6, while that of V2 remains 5. The reduced cluster possesses two V−O$^{(2)}$−Al and two V−O$^{(3)}$−V,Al^1 bonds; i.e., upon reduction two V−O$^{(2)}$−Al bonds are given up, and a new V−O$^{(3)}$−V,Al bond has formed (cf. section 4.1). The resulting V$_2$O$_4$ cluster binds as much as possible to the α-Al$_2$O$_3$ surface, and the total number of V−O and O−Al bonds between the cluster and the surface is the same as in the L1 cluster. Hence, it is no surprise that the binding energy with respect to the most stable (cyclic trans) V$_2$O$_4$ gas-phase cluster, 6.77 eV, is very similar to the binding energy of the L1 cluster itself, 6.80 eV.

Upon removal of the 2-fold coordinated O3 and O4 atoms bound to the V2 site, the relaxations are smaller (∼1 eV, Table 6), and the resulting structures are similar to the unrelaxed ones. The removal of the O4 atom is by ∼1.2 eV more difficult. Figure 6 shows the final linear L1−O3 structure. The defect formation energy is 3.31 eV, and the adsorption energy with respect to the (also linear) OVOV(O)O gas phase cluster is 8.02 eV. This linear cluster binds more strongly to the surface than the cyclic one because it is coordinatively more unsaturated. As a result, the stability difference between the linear (L1−O3) and cyclic (L1−O1) structure is smaller on the surface ($\Delta E_{ad} = 0.52$ eV, cf. Table 6) than in the gas phase (1.77 eV, cf. Table 2). A linear surface cluster is also obtained upon removal of the vanadyl oxygen atom from the L2 cluster (L2−O4, cf. Figure 6). This reduction has a similar energy cost as L1−O3 (3.77 eV) and is accompanied by small relaxations only (∼0.3 eV).

Removing the O5 atom from the V−O$^{(2)}$−V bridge of the L2 cluster yields two monomeric VO$_2$ species (L2−O5) with the vanadium atoms above Al^4 atoms (Figure 6). Because of a large relaxation effect (1.77 eV), it requires 3.70 eV. The

coordination of both V1 and V2 decreases by one. The V2 atom, initially above an oxygen atom of the support, moves above an octahedral site following the Al$_2$O$_3$ stacking, and the monomeric units become further separated from each other. The two VO$_2$ monomers in the L2−O5 cluster are 0.07 eV more stable than the linear L2−O4 cluster, while in the gas phase they are 2.94 eV less stable (cf. Table 2). The stabilizing effect of the surface is largest for the species with the lowest coordination in the gas phase, as already mentioned.

Two VO$_2$ monomers are also obtained when the bridging 3-fold coordinated O5 atom is removed from L1, but relaxation is smaller (0.58 eV) and the reduction more difficult (defect formation energy 4.75 eV) with one O atom of each VO$_2$ coordinated to the same surface Al atom (see figure in Supporting Information).

Removal of the 2-fold coordinated oxygen atoms O1, O2, and O3 from the V−O$^{(2)}$−Al interface bonds of the L2 cluster costs ∼4.4−4.8 eV with relaxation contributions within the 0.7−1.0 eV range. The resulting structures are shown in the Supporting Information.

Summarizing, among the oxygen atoms in the V$_2$O$_5$ surface clusters L1 and L2 the least bound are the bridging O1/O2 and O3 atoms of the V−O$^{(2)}$−Al^1 interface of the L1 cluster. Their removal requires 2.79/2.80 and 3.31 eV, respectively, while 3.77 and 3.70 eV are required to remove the O atom from the O$^{(1)}$=V group and the V−O$^{(2)}$−V bridge of the L2 cluster, respectively. The latter is comparable to that of removing O$^{(2)}$ atoms from the (001) surface, which is 3.6−3.7 eV.[21]

We now turn to the electronic structure of the reduced clusters. Upon oxygen removal two electrons are left in the system. They occupy d states localized either on one or on both V atoms. Thus, reduction yields either a V^{III}(d^2)/V^V(d^0) situation or a V^{IV}(d^1)/V^{IV}(d^1) pair. The ground state of all reduced systems is a triplet. Figure 7 shows the spin density projected on the vanadium d states (DOS), n(d$_{up}$)−n(d$_{down}$), for selected reduced clusters, namely L1−O1, L1−O3, L2−O4, and L2−O5. The peaks right below the Fermi level result from the partial occupation of vanadium 3d states. The integral of these spin-projected DOS reflects that removal of the 2-fold coordinated O1 atom from the L1 cluster yields a pair of V^{IV} centers with populations of ∼0.93−0.97 d electrons for both V sites. Similarly, a pair of V^{IV} centers is obtained when the V−O$^{(2)}$−V bridging oxygen atom is removed from L2 (L2−O5), but the two V^{IV} centers are not equivalent. In contrast, for L1−O3 and L2−O4 the d-projected spin densities show a V^{III} center with the two electrons localized at the V2-site.

The results of the DOS analysis show that, for those systems for which reduction induces large relaxations, a pair of V^{IV} centers is formed (cf. L1−O1, L1−O2, L2−O5). For the L1−O1 and L1−O2 clusters these relaxations lead to formation of a new V−O−V bond. This is similar to the reduction of the single crystal V$_2$O$_5$(001) surface.[21]

For the gas-phase clusters we have an analogous situation. The reduction of the cyclic V$_2$O$_5$ cluster leading to the cyclic trans cluster costs 2.77 eV, whereas forming the less stable linear OVOV(O)O cluster costs 4.53 eV (cf. Table 6). The latter has a V^{III}(d^2)V^V(d^0) electronic structure with a triplet ground state, while the cyclic trans cluster has an additional V−O−V bond with a V^{IV}(d^1)V^{IV}(d^1) pair with the d^1 electrons antiferromagnetically coupled (singlet open-shell state).

E. Vibrational Analysis. Vibrational spectroscopy is a useful tool for structural characterization,[11,48−52] but the interpretation of the measured spectra is not always straightforward.[11,53] We report the vibrational frequencies of the two most stable V$_2$O$_5$/

Vanadium Oxides on Aluminum Oxide Supports

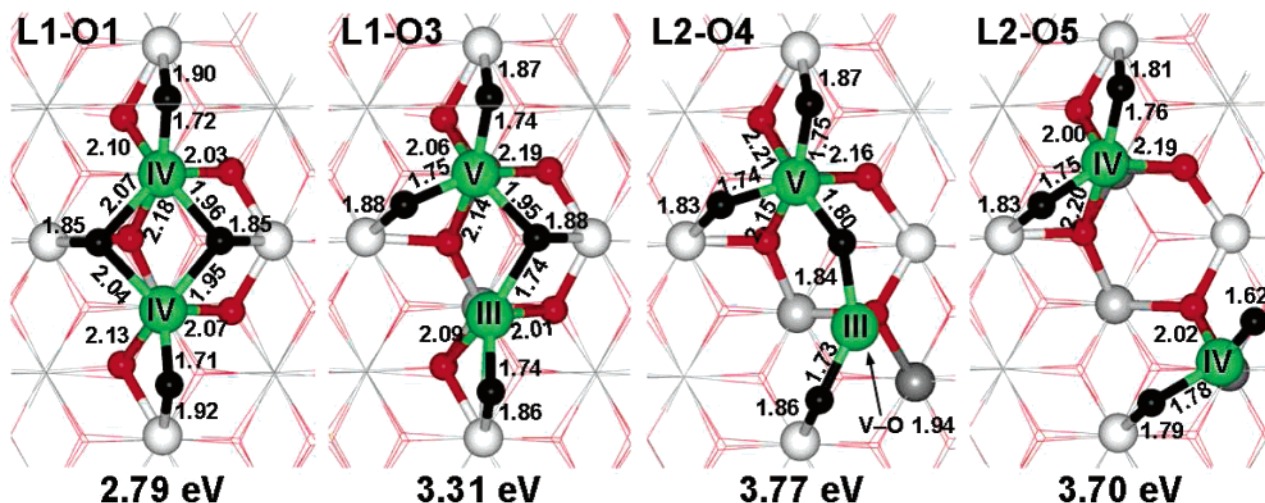*J. Phys. Chem. B, Vol. 109, No. 49, 2005* **23539**

Figure 6. Optimized structures of the selected reduced clusters of Figure 4, which were created from the L1 and L2 clusters. The labeling of the removed atom (Oi) corresponds to that in Figure 4. The color code is the same as in Figure 2. Bond lengths are in Å.
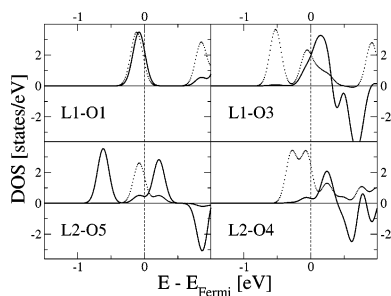

Figure 7. Spin density n(d$_{up}$)−n(d$_{down}$) projected on d states of V atoms in reduced L1−Oi and L2−Oi clusters (cf. Figure 6). The labeling of the removed atom (Oi) corresponds to that in Figure 4. Solid line, V1; dashed line, V2. For labeling of atoms see Figure 4.

Al$_2$O$_3$ systems and compare with other VO$_x$/Al$_2$O$_3$ model systems. The (2 × 2) surface unit cell of the supported V$_2$O$_5$ clusters contains 127 atoms, which means that the vibrational spectra will have 378 optical and 3 acoustic modes.

For both clusters all resulting frequencies are real which shows that the structures are minima. The three lowest frequencies, which should be zero, are less than 10 cm^{-1}, which is well within the range of numerical error. Tests have been made to see how much the frequencies are shifted if the atoms in the bottom of the slab (up to four Al−O$_3$−Al trilayers) are fixed. Fixing half of the slab (three Al−O$_3$−Al trilayers) causes a shift of at most 1 cm^{-1} in the resulting frequencies (see Table 8). Fixing one additional trilayer caused a shift of up to 4 cm^{-1} in the region of interest. Therefore, the results described below correspond to calculations with the bottom three trilayers of the alumina slab fixed. For the calculation with no fixed atoms, vibrations located at the bottom of the slab correspond to vibrations of the clean α-Al$_2$O$_3$(0001) surface. Those parallel to a surface would not be visible in an IR spectrum.

The spectrum of the most stable adsorbed cluster (L1) has lines in the 76−922 cm^{-1} range without large gaps. The highest frequency modes (922−803 cm^{-1}) involve a few atoms, namely the V$_2$O$_5$ unit and the support atoms localized at the surface (i.e., within the outermost Al−O$_3$−Al−Al atomic layers), while in all others mostly all atoms of the slab participate. Table 7 shows the calculated highest frequencies.

The vibration at 922 cm^{-1} is an in-phase stretching of the two short V−O$^{(2)}$(−Al) bonds (1.67 and 1.68 Å). It involves deformations of the corresponding V−O$^{(2)}$−Al angles, but only Al^1 atoms of the first layer are involved. This is the only

observable line in the whole spectrum that is characteristic of the adsorbed clusters. The lower lying peaks caused by V−O stretching (cf. Table 8) are "hidden" in the more intense peak at 845 cm^{-1}, caused by stretchings of the surface Al−O bonds in the outermost Al−O$_3$−Al−Al atomic layers.

With decreasing energy of the vibrations more Al and O layers contribute to the vibrations, and below 760 cm^{-1} the whole slab vibrates. Down to about 560 cm^{-1} the stretching modes dominate the vibrations. At lower wavenumbers there is an increasing participation of deformations, and below ∼350 cm^{-1} the vibrations are pure deformations.

Table 8 lists the highest vibrational frequencies of the L2 system. In this calculation the bottom three Al−O$_3$−Al trilayers were fixed. Here the band at 1059 cm^{-1} arises from the vanadyl bond stretch. This is lower than obtained for the V$_2$O$_5$(001) surface (1085−1102 cm^{-1} for the model from ref 21 and the same computational setup as used here; 1079−1095 cm^{-1}, ref 14) and within the range of vanadyl-terminated vanadia films on alumina (1058, 1076 cm^{-1}, ref 14). Thus, the position of the vanadyl band cannot be used to discriminate between small clusters and thin films of vanadia on alumina.

In this system the V−O$^{(2)}$ bonds are shorter than in L1, and the vibrations caused by their stretching lie lower than for L1 (cf. 922 and 871 cm^{-1}). The V−O$^{(2)}$ stretches are also coupled to Al−O stretching more than in the case of the L1 system. The V−O$^{(2)}$ stretching modes (cf. Table 8) are again not distinguishable in the spectrum because the lines caused by Al−O stretching are more intense. For example, the line at 871 cm^{-1} forms a broader peak together with a more intense line (863 cm^{-1}) caused by Al−O stretching.

Figure 8 shows the calculated harmonic spectra of the L1 and L2 systems as well as that of the α-Al$_2$O$_3$(0001) surface. The broad intense peak between 700 and 800 cm^{-1} in all the spectra corresponds to alumina vibrations. This peak is shifted by the adsorbed cluster by ∼30 cm^{-1} with respect to the clean α-Al$_2$O$_3$ surface.

We have already shown in a previous study[14] that V−O−(Al) bonds with 3-fold coordinated oxygen atoms do not give rise to bands higher than 805 cm^{-1} (cf. Figure 9). In this work, the highest V−O−(Al) vibration at 922 cm^{-1} arises from the presence of short V−O$^{(2)}$ bonds at the interface. In bulk AlVO$_4$, the shortest V−O$^{(2)}$−(Al) bonds are also 1.67 Å long (ref 53), but the corresponding stretching frequencies are in the 1025−882 cm^{-1} range. In this system, however, the V−O$^{(2)}$(−Al)

TABLE 7: Vibrational Frequencies (in cm^{-1}) for the L1 System

	no. fixed bottom trilayers			
0	3	4		description
949−947				3 lines, back of the slab, parallel to surface
922	922 (2.2)^c	922		V−O$^{(2)}$ short bonds in-phase str
919−905				5 lines, back of the slab, parallel to surface
882	882 (0.3)	882		V−O$^{(2)}$ short bonds out-of-phase str + 1 V−O$^{(2)}$ long bond str
876	876 (0.2)	874		alumina surface^a
867	866 (1.4)	866		V−O$^{(2)}$ long bonds in-phase str + 1 V−O$^{(2)}$ short bond str
845	844 (8.3)	843		alumina surface^b
837	837 (2.8)	835		alumina surface^b
834	834 (0.1)	832		V−O$^{(2)}$ long bonds out-of-phase str + V−O$^{(2)}$ short bonds str
816	815 (0.1)	812		alumina surface^b + 1 long V−O$^{(2)}$(−Al) bond str
803	803 (0.2)	800		alumina surface^b

^{a} Al−O vibrations within the outermost Al−O$_3$−Al−Al atomic layers. ^{b} Vibrations of all (nonfixed) Al−O bonds. ^{c} Relative IR intensities are given in parentheses.

TABLE 8: Vibrational Frequencies (in cm^{-1}) for the L2 System

wavenumber	description
1059 (4.2)	V=O$^{(1)}$ str
897 (2.1)	alumina surface^a
871 (2.5)	alumina surface^b + V2−O$^{(2)}$(−Al) str
863 (6.6)	alumina surface^b
857 (0.1)	alumina surface^b
837 (0.2)	V2−O$^{(2)}$(−Al) str
830 (0.4)	alumina surface^b
817 (8.4)	V2−O$^{(2)}$(−Al) str + V1−O$^{(2)}$−V2 str alumina surface^b
810 (0.0)	V2−O$^{(2)}$(−Al) str + alumina surface^b
800 (2.6)	alumina surface^b + V1−O$^{(2)}$(−Al) str
794 (8.7)	alumina surface^b + V2−O$^{(2)}$(−Al) str
788 (100)	Al$_2$O$_3$ support^b
773 (10.1)	Al$_2$O$_3$ support^c + V2−O$^{(2)}$(−Al) str

^{a} Al−O vibrations within the outermost Al−O$_3$−Al−Al atomic layers. ^{b} Vibrations of all (nonfixed) Al−O bonds.

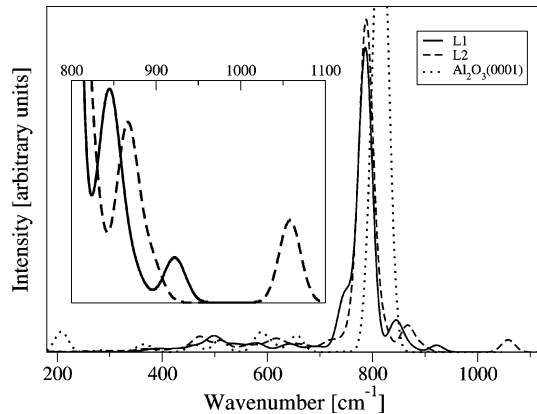**Figure 8.** Harmonic vibrational frequencies of the L1 and L2 clusters and the α-Al$_2$O$_3$(001) frequencies. The IR intensities are calculated from the change in the component of the dipole moment perpendicular to the surface. The lines were broadened by Gaussian functions. Inset: spectra of L1 and L2 between 800 and 1100 cm^{-1}.

bonds belong to rings composed of alternating metal and oxygen atoms leading to highly coupled vibrations. The present results and those for AlVO$_4$ support the previous assignment[11] of the observed band at 941 cm^{-1} for vanadia particles on alumina[9] to V−O−Al interface modes. It is likely that 2-fold coordinate oxygen atoms are present at the interface.

F. Thermodynamical Stability of Different Surfaces. Supported vanadia aggregates are prepared by evaporation of metallic vanadium in an oxygen ambient (see e.g. ref 9). We have used statistical thermodynamics to take into account the effects of temperature, oxygen pressure, and vanadium concentration on the stability of differently terminated V$_n$O$_m$ films with
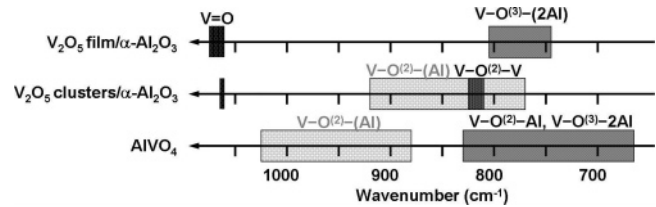

Figure 9. Harmonic vibrational frequencies of alumina-supported thin vanadia films,[14] alumina-supported V$_2$O$_5$ clusters (L1, L2), and bulk AlVO$_4$ (ref 53).

varying thickness.[15] In this work, we include results for all V$_2$O$_5$ and V$_2$O$_4$ (i.e., reduced) supported clusters and discuss the stability of systems that would represent the formation of dispersed dimeric vanadia units on the alumina support. The procedure has been described in detail in ref 54, and we follow closely the notation of ref 15.

We consider the equilibrium reaction

$$n\text{V} + m\frac{1}{2}\text{O}_2 + \text{Al}_2\text{O}_3(0001) \rightleftharpoons \text{V}_n\text{O}_m/\text{Al}_2\text{O}_3 \qquad (3)$$
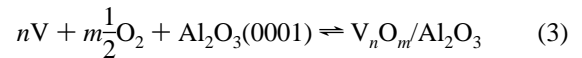
The corresponding reaction energy is

$$\Delta E = E^{\text{V}_n\text{O}_m/\text{Al}_2\text{O}_3} - E^{\text{Al}_2\text{O}_3(0001)} - nE_{\text{V}} - \frac{m}{2}E_{\text{O}_2} \qquad (4)$$

where $E^{\text{V}_n\text{O}_m/\text{Al}_2\text{O}_3}$ is the total energy of the slab with a given composition and structure and $E^{\text{Al}_2\text{O}_3(0001)}$ is the total energy of the clean α-Al$_2$O$_3$ support, respectively. n and m are the number of V and O atoms of the supported particle, respectively. E_{V} and E_{O_2} are total energies of metallic bcc bulk vanadium and the free oxygen molecule, respectively. We can express the chemical potentials of V and O as

$$\mu V(T,a_{\text{V}}) = E_{\text{V}}^{\text{bulk}} + \Delta\mu_{\text{V}}(T,a_{\text{V}}) \qquad (5)$$

$$\frac{1}{2}\mu_{\text{O}_2}(T,p) = E_{\text{O}_2} + \Delta\mu_{\text{O}_2}(T,p) \qquad (6)$$

where a_{V} is the vanadium activity and p the oxygen partial pressure. Now the change in the surface free energy accompanying the reaction can be expressed as

$$\Delta\gamma(T,p) = \frac{1}{A}[\Delta E - n\Delta\mu_{\text{V}} - m\Delta\mu_{\text{O}_2}] \qquad (7)$$

The Gibbs free energies of the Al$_2$O$_3$(0001) surface and the V$_n$O$_m$/Al$_2$O$_3$ supported cluster components have been approximated by the calculated DFT total energies at zero temperature (T) and at a given unit cell volume V. This means
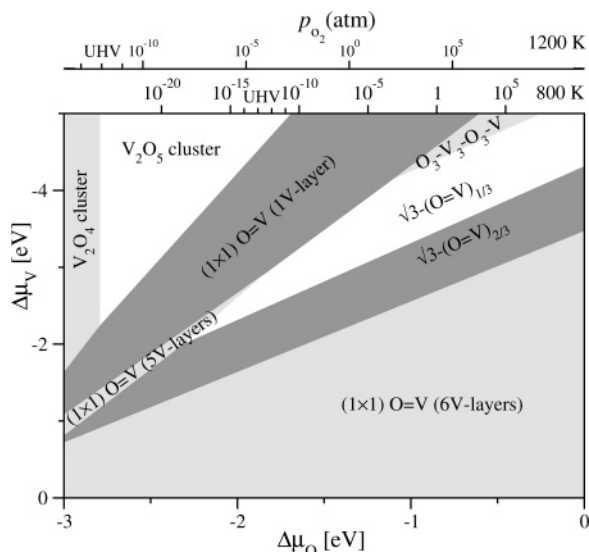
Vanadium Oxides on Aluminum Oxide Supports

J. Phys. Chem. B, Vol. 109, No. 49, 2005 **23541**

Figure 10. Phase diagram as a function of the chemical $\Delta\mu_O$ and $\Delta\mu_V$ for alumina-supported V_nO_m clusters and films (ref 15). $\Delta\mu_O$ is translated into a pressure scale at $T = 800$ and 1200 K.

that contributions depending on vibrational states of the systems and those resulting from the pV term are neglected. A is the area of the surface unit cell.

Using eq 7, we predict which surface structure is the most stable by searching for the model with the lowest surface free energy $\Delta\gamma$ for given $\Delta\mu_O$ and $\Delta\mu_V$ values. It is understood that the V and O particle reservoirs are in equilibrium with (metallic) bulk V and O_2 in the (ideal) gas phase so that $\Delta\mu_{O_2}$ and $\Delta\mu_V$ at a given temperature depend on O_2 pressure and V activity.[15] The latter is related to the concentration through the activity coefficient γ_V.[55] Figure 10 shows the result, together with those for the supported films of ref 15.[56]

Under reducing conditions (UHV and 800 K) and when the vanadium concentration is low, the calculations favor the formation of V_2O_5 dispersed clusters without vanadyl oxygen atoms. However, the cluster with a vanadyl oxygen is only marginally less stable. (The energy difference of 0.12 eV implies that at 800 K 18% of the clusters have the L2 structure.) As the V concentration increases, supported vanadia films become more stable. Initially, an ultrathin ($\lesssim 2$ Å) film forms that is fully covered with vanadyl oxygen atoms. For higher V concentrations, thicker, bulklike V_2O_3 films are stable, for which different film terminations are possible for different conditions (see ref 15).

An important difference between the vanadia clusters and the extended films is the stability of the reduced systems. The phase diagram indicates that vanadyl groups terminating the films are thermally stable up to at least 1200 K in UHV.[14] A recent experimental study on thick $V_2O_3(0001)$ films[57] found a similar thermal behavior of V=O groups.

In contrast, reduced clusters such as L1−O1 would become stable at this temperature in UHV (at 1200 K a pressure of 10^{-12} atm corresponds to $\Delta\mu_O \approx -2.8$ eV). This correlates with the more facile reduction (discussed in section 4.4) of the cluster on the $Al_2O_3(0001)$ surface compared to supported films (see Table 6).

V. Comparison and Conclusions

The most stable supported V_2O_5 cluster on the α-$Al_2O_3(0001)$ surface is nearly an "extension" of the bulk corundum structure, i.e., oxygen atoms follow the hexagonal stacking of the oxygen layers, while both V atoms occupy octahedral interstitial sites.

It does not have any vanadyl oxygen atoms as those terminating vanadia films; however, the system contains V−$O^{(2)}$−Al sites (that are not present at the film/support interface). It is the existence of these sites (with their $1.67-1.68$ Å V−O bonds) which gives rise to V−O stretching frequencies up to 922 cm^{-1}. For the epitaxial films and α-Al_2O_3 there are no frequencies higher than 805 cm^{-1} except for the vanadyl bond stretch. This result provides further support for the assignment[11] of the band observed around 941 cm^{-1} for vanadia particles on alumina[9] to the V−O−Al interface mode. The nature of the vanadia−support interface is different for small particles (i.e., clusters) and epitaxial films, as differently coordinated sites are involved (V−$O^{(2)}$−Al compared to e.g. V−$O^{(3)}$−Al_2), and this yields to differences in the "anchoring" support effect (that hinders the vacancy formation).

We have determined the thermodynamic stability of V_2O_5 and V_2O_4 (i.e., reduced) supported species relative to differently terminated vanadia films of varying thickness,[15] depending on the oxygen pressure and amount of evaporated vanadium at a given temperature. At low V concentration, dispersed V_2O_5 units may cover the surface occupying positions that resemble "epitaxial growth". Increasing the V loading can lead to formation of films (or wider and thicker particles) for which the presence of vanadyl terminating species is a predominant feature as those observed in ref 9.

Removal of 2-fold coordinated oxygen atoms at the cluster/alumina interface is facilitated by lattice relaxation that leads to formation of an additional V−O−V bond and lowers the energy by about 2.5 eV. As a result, pairs of V^{IV} centers are formed. This is similar to removal of surface vanadyl oxygen atoms on the single-crystal $V_2O_5(001)$ surface,[21] where the formation of additional V−O−V bonds between the crystal layers lowers the energy by ∼2.0 eV (cf. Table 6). As a result, the defect formation energy (2.79 eV) for a V_2O_5 cluster on α-$Al_2O_3(0001)$ is about 0.9 eV larger than for the $V_2O_5(001)$ single-crystal surface (1.93 eV). However, it is ∼1.3 eV lower than for a vanadyl-terminated ultrathin film,[15] for which no large relaxation is possible and a $V^{III}(d^2)$ site is created.

In summary, if we accept that the catalytic activity of a vanadia catalyst depends on its reducibility (the catalyst donates an oxygen atom in oxygenation reactions or it uses an oxygen atom in oxidative dehydrogenation reactions), we may take the energy of oxygen defect formation as an indicator of catalytic activity. We have previously shown that a thin film on an α-$Al_2O_3(0001)$ support is much less reactive than the (001) surface of crystalline vanadia because there is no way of stabilizing the defect by forming new bonds. Here we have shown that small (V_2O_5) vanadia clusters on α-$Al_2O_3(0001)$ are still more difficult to reduce than the (001) V_2O_5 crystal surface, but significantly easier than thin films. The reason is that a new V−O−V bond is formed when the defect is created at the V−$O^{(2)}$−Al interface site.

Supporting Information Available: Optimized structures of V_2O_4 clusters obtained by O removal from the L1 and L2 clusters that are not shown in Figure 6: L1−O2, L1−O4, L1−

O5, L2−O1, L2−O2, and L2−O3. This material is available free of charge via the Internet at http://pubs.acs.org.

References and Notes

(1) Weckhuysen, B. M.; Keller, D. E. *Catal. Today* **2003**, *78*, 25.

(2) Bond, G. C.; Tahir, S. F. *Appl. Catal.* **1991.** *71*, 1.

(3) Bañares, M. A. *Catal. Today* **1999**, *51*, 319.

(4) Kondratenko, E. V.; Buyevskaya, O. V.; Baerns, M. *Top. Catal.* **2001**, *15*, 175.

(5) Wachs, I. E.; Deo, G.; Juskelis, M. V.; Weckhuysen, B. M. In *Dynamics of Surfaces and Reaction Kinetics in Heterogeneous Catalysis*; Froment, G. F., Waugh, K. C., Eds.; Elsevier: Amsterdam, 1997; Vol. 109, p 305.

(6) Deo, G.; Wachs, I. E.; Haber, J. *Crit. Rev. Surf. Chem.* **1994**, *4*, 141.

(7) Bond, G. C. *Appl. Catal., A* **1997**, *157*, 91.

(8) Biener, J.; Baumer, M.; Madix, R. J.; Liu, P.; Nelson, E. J.; Kendelewicz, T.; Brown, G. E. *Surf. Sci.* **1999**, *441*, 1.

(9) Magg, N.; Giorgi, J. B.; Schroeder, T.; Bäumer, M.; Freund, H.-J. *J. Phys. Chem. B* **2002**, *106*, 8756.

(10) Magg, N.; Giorgi, J. B.; Frank, M. M.; Immaraporn, B.; Schroeder, T.; Bäumer, M.; Freund, H.-J. *J. Am. Chem. Soc.* **2004**, *126*, 3616.

(11) Magg, N.; Immaraporn, B.; Giorgi, J. B.; Schroeder, T.; Bäumer, M.; Döbler, J.; Wu, Z.; Kondratenko, M.; Cherian, E.; Baerns, M.; Stair, P. C.; Sauer, J.; Freund, H.-J. *J. Catal.* **2004**, *226*, 88.

(12) Kulawik, M.; Nilius, N.; Rust, H.-P.; Freund, H.-J. *Phys. Rev. Lett.* **2003**, *91*, 256101.

(13) Kresse, G.; Schmid, M.; Napetschnig, E.; Shishkin, M.; Köhler, L.; Varga, P. *Science* **2005**, *308*, 1440.

(14) Brázdová, V.; Ganduglia-Pirovano, M. V.; Sauer, J. *Phys. Rev. B* **2004**, *69*, 165420.

(15) Todorova, K. T.; Ganduglia-Pirovano, M. V.; Sauer, J. *J. Phys. Chem. B* **2005**, *109*, 23523.

(16) Calatayud, M.; Mguig, B.; Minot, C. *Surf. Sci.* **2003**, *526*, 297.

(17) Calatayud, M.; Mguig, B.; Minot, C. *J. Phys. Chem. B* **2004**, *108*, 15679.

(18) Calatayud, M.; Mguig, B.; Minot, C. *Surf. Sci. Rep.* **2004**, *55*, 169.

(19) Vittadini, A.; Selloni, A. *J. Phys. Chem. B* **2004**, *108*, 7337.

(20) Vittadini, A.; Casarin, M.; Selloni, A. *J. Phys. Chem. B* **2005**, *109*, 1652.

(21) Ganduglia-Pirovano, M. V.; Sauer, J. *Phys. Rev. B* **2004**, *70*, 045422.

(22) Perdew, J. P. In *Electronic Structure of Solids '91*; Ziesche, P., Eschrig, H., Eds.; Akademie Verlag GmbH: Berlin, 1991.

(23) Perdew, J. P.; Chevary, J. A.; Vosko, S. H.; Jackson, K. A.; Pederson, M. R.; Singh, D. J.; Fiolhais, C. *Phys. Rev. B* **1992**, *46*, 6671.

(24) Kresse, G.; Hafner, J. *Phys. Rev. B* **1993**, *48*, 13115.

(25) Kresse, G.; Furthmüller, J. *Phys. Rev. B* **1996**, *54*, 11169.

(26) Blöchl, P. E. *Phys. Rev. B* **1994**, *50*, 17953.

(27) Kresse, G.; Joubert, D. *Phys. Rev. B* **1999**, *59*, 1758.

(28) Monkhorst, H. J.; Pack, J. D. *Phys. Rev. B* **1976**, *13*, 5188.

(29) Kirfel, A.; Eichhorn, K. *Acta Crystallogr.* **1990**, *A46*, 271.

(30) Manassidis, I.; Gillan, M. *J. Am. Ceram. Soc.* **1994**, *77*, 335.

(31) Blonski, S.; Garofalini, S. H. *Surf. Sci.* **1993**, *295*, 263.

(32) Renaud, G. *Surf. Sci. Rep.* **1998**, *32*, 1.

(33) Sauer, J.; Vyboishchikov, S. F. *J. Phys. Chem. A* **2000**, *104*, 10913.

(34) Vyboishchikov, S. F.; Sauer, J. *J. Phys. Chem. A* **2001**, *105*, 8588.

(35) Calatayud, M.; Andrés, J.; Beltrán, A. *J. Phys. Chem. A* **2001**, *105*, 9760.

(36) Sauer, J.; Döbler, J. *Dalton Trans.* **2004**, *19*, 3116.

(37) Pykavy, M.; van Wüllen, C.; Sauer, J. *J. Chem. Phys.* **2004**, *120*, 4207.

(38) Herzberg, G. *Molecular Spectra and Molecular Structure. I. Spectra of Diatomic Molecules*, 2nd ed.; Robert E. Krieger Publishing Co.: Malabar, FL, 1989.

(39) Perdew, J. P.; Burke, K.; Ernzerhof, M. *Phys. Rev. Lett.* **1996**, *77*, 3865.

(40) Zhang, Y.; Yang, W. *Phys. Rev. Lett.* **1998**, *80*, 890.

(41) The system was first let to evolve at 700 K for 0.5 ps, with a time step of 1 fs. Afterward, it was annealed to 20 K in 2.5 ps with a time step of 5 fs. The structure was finally reoptimized at 0 K. All the calculations were done at 250 eV with ultrasoft pseudopotentials.

(42) Vanderbilt, D. *Phys. Rev. B* **1990**, *41*, 7892.

(43) Chen, K.; Khodakov, A.; Yang, J.; Bell, A. T.; Iglesia, E. *J. Catal.* **1999**, *186*, 325.

(44) Chen, K.; Iglesia, E.; Bell, A. T. *J. Catal.* **2000**, *192*, 197.

(45) Chen, K.; Bell, A. T.; Iglesia, E. *J. Phys. Chem. B* **2000**, *104*, 1292.

(46) Argyle, M. D.; Chen, K.; Resini, C.; Krebs, C.; Bell, A. T.; Iglesia, E. *Chem. Commun.* **2003**, *16*, 2082.

(47) Argyle, M. D.; Chen, K.; Resini, C.; Krebs, C.; Bell, A. T.; Iglesia, E. *J. Phys. Chem. B* **2004**, *108*, 2345.

(48) Wachs, I. E. *Catal. Today* **1996**, *27*, 437.

(49) Hardcastle, F. D.; Wachs, I. E. *J. Phys. Chem.* **1991**, *95*, 5031.

(50) Turek, A. M.; Wachs, I. E. *J. Phys. Chem.* **1992**, *96*, 5000.

(51) Deo, G.; Wachs, I. E. *J. Phys. Chem.* **1991**, *95*, 5889.

(52) Briand, L. E.; Jehng, J.-M.; Cornaglia, L.; Hirt, A. M.; Wachs, I. E. *Catal. Today* **2003**, *78*, 257.

(53) Brázdová, V.; Ganduglia-Pirovano, M. V.; Sauer, J. *J. Phys. Chem. B* **2005**, *109*, 394.

(54) Zhang, W.; Smith, J. R.; Wang, X.-G. *Phys. Rev. B* **2004**, *70*, 024103.

(55) *Materials Thermochemistry*, 6th ed.; Kubaschewski, O., Alcock, C. B., Spencer, P. J., Eds.; Pergamon Press: Oxford, 1993.

(56) Note that the PW91 functional generally overestimates formation and binding energies, so that the calculated chemical potentials may be shifted by several 100 meV. Therefore, the absolute O partial pressure and the V activity may change by 2−3 orders of magnitude. Nevertheless, the overall trend and the dependence of different surface structures on a_V and oxygen pressure are valid.

(57) Dupuis, A.-C.; Abu Haija, M.; Richter, B.; Kuhlenbeck, H.; Freund, H.-J. *Surf. Sci.* **2003**, *539*, 99.